

Pion-nucleus single-charge exchange above the resonance

E. Oset

Departamento Fisica Teorica and Instituto de Fisica Corpuscular, Centro Mixto Universidad de Valencia Consejo Superior de Investigaciones Científicas, E-46100 Burjassot (Valencia), Spain

D. Strottman

Theoretical Division, Los Alamos National Laboratory, Los Alamos, New Mexico 87545

(Received 23 July 1990)

The excitation function for the (π^+, π^0) reaction on ${}^7\text{Li}$ and ${}^{14}\text{C}$ to analog states in ${}^7\text{Be}$ and ${}^{14}\text{N}$ in the range of 250 to 650 MeV pion kinetic energy is calculated. The Glauber model with microscopic shell-model wave functions is used. The effects of antisymmetry and spin flip were explicitly evaluated; experimental πN partial waves up to $l=3$ were included in the calculation. The calculated cross section is too large compared to experiment. The effects of two- and three-body pion absorption are calculated and found to reduce the calculated cross section by a small amount to values nearer experiment.

I. INTRODUCTION

Recent experiments¹ of the (π^+, π^0) reaction on nuclei have extended measurements of the pion-induced single-charge exchange reaction (SCX) into the hitherto unexplored energy regime above the $\Delta(3,3)$ resonance. These experiments found that the cross section at forward angles increases with increasing energy of the projectile, in contrast with the behavior of single-charge exchange on a free nucleon. It is the purpose of this article to demonstrate that this behavior may be qualitatively understood, and that the surprising but understandable aspect of the reaction is not that it is large, but rather that it is relatively small.

One may obtain a qualitative understanding of the apparent anomalous behavior of the excitation function by considering the competition between distortion and charge exchange on a single nucleon. In the region of the $(3,3)$ resonance, pions are strongly absorbed and the SCX reaction is correspondingly suppressed. As one moves higher in energy away from the $(3,3)$ resonance, the amplitude for charge exchange on a free nucleon slowly decreases, but the distortion of the pion wave rapidly decreases. The actual calculated forward-scattering cross section can only be determined by more quantitative, detailed considerations, but this argument suggests it should not be surprising that the SCX reaction on a nucleus will have a much different energy dependence than on a free nucleon.

In the energy of the resonance and below, only the s and p partial waves need to be included in calculations. However, above the resonance additional partial waves need to be included in calculations. An examination of the FP84 phase-shift solution of Arndt, Ford, and Roper² demonstrates the D_{31} phase shift becomes important above 250 MeV pion energy and the F_{51} should be included above 450 MeV. Thus the usual programs used to calculate pion-induced reactions at lower energies and which are based on the dominance of the s and p waves are not applicable in this higher-energy regime.

In this paper we generalize our previous work on the Glauber model³ to include an arbitrary number of partial waves. In addition, we generalize the Glauber formalism to account for pion absorption. The standard Glauber approach takes into account distortion of the pion wave due to multiple scattering; however, it ignores higher-order processes, particularly pion absorption. Pion absorption in the energy domain relevant to our calculations occurs dominantly on two nucleons, although absorption on three or more nucleons can be important. We show that a proper understanding of the SCX reaction in the energy region of 300–600 MeV kinetic energy requires the inclusion of pion absorption.

In Sec. III we show the results of SCX on ${}^{14}\text{C}$; the calculated results are significantly larger than experiment. In Sec. III we discuss our model for including pion absorption into the Glauber model, and Sec. IV contains a derivation of the model used to account for absorption. Section V contains results of calculations and Sec. VI conclusions. Some preliminary versions of these results were presented earlier.⁴

II. FORMALISM

In this paper we shall use the Glauber model,³ which has the advantage of being microscopic and allowing physical intuition, yet has been found to provide reliable estimates of cross sections at resonance energies. With increasing pion energies, the model should be increasingly more accurate as the πN cross section becomes increasingly forward peaked. In our microscopic version of the Glauber model, the effects of higher partial waves may be explicitly included. At the pion energies with which we are dealing, the pion is less strongly absorbed than at the resonance and details of nuclear structure are important. The Glauber model allows the use of arbitrarily complicated shell-model wave functions; hence correlations are automatically included.

The SCX amplitude in the Glauber approach may be written as⁵

$$F(q) = \frac{ik}{2\pi} \int d^2b e^{iq \cdot b} \left\langle \Psi_f, J_f, M_f \left| \sqrt{2} \sum_i \Gamma_i^{(v)} \tau_i^+ \prod_{j \neq i} (1 - \Gamma_j^{(s)}) \right| \Psi_i, J_i, M_i \right\rangle, \quad (1)$$

where Γ_j is the π -nucleon profile function

$$\Gamma_j(\mathbf{b} - \mathbf{s}_j) = \frac{1}{2\pi ik} \int d^2q h(q) e^{-iq \cdot (\mathbf{b} - \mathbf{s}_j)}, \quad (2)$$

obtained from the πN amplitude, which we take to be of the form

$$h(q) = f(q) + ig(q) \boldsymbol{\sigma} \cdot \hat{\mathbf{n}}. \quad (3)$$

Each of the amplitudes f and g may be written as the sum of an isoscalar and an isovector term, e.g.,

$$f(q) = f^{(s)}(q) + \boldsymbol{\Theta} \cdot \boldsymbol{\tau} f^{(v)}(q), \quad (4)$$

and similarly for g . In Eq. (4), $\boldsymbol{\Theta}$ is the isospin operator of the pion and $\boldsymbol{\tau}$ the ordinary isospin Pauli matrices, $J_i, M_i, J_f,$ and M_f are the initial and final total angular momenta and their M projections. In Eqs. (1) and (4) the superscripts s and v refer to isoscalar and isovector, respectively. The theoretical cross sections are obtained by averaging over initial and summing over the final-state angular momentum projections.

The non-spin-flip amplitudes in each isospin channel are obtained from

$$f = \sum_l [(l+1)f_{l+} + lf_{l-}] P_l(\cos\theta),$$

the spin-flip amplitudes are

$$g = \sum_l (f_{l+} - f_{l-}) P_l'(\cos\theta) \sin\theta,$$

and the subscripts l_{\pm} refer to the angular momentum $j = l \pm \frac{1}{2}$ of each partial wave. From the above equations we see that

$$f^{(s)} = \frac{2f_{3/2} + f_{1/2}}{3}, \quad f^{(v)} = \frac{f_{3/2} - f_{1/2}}{3},$$

where the subscript refers to isospin and we have temporarily omitted the reference to the partial wave l, j .

Since the operator in Eq. (1) is a product of A one-body operators, if the shell-model wave functions are determinants, then the evaluation of the matrix elements of Eq. (1) reduces to the evaluation of an $A \times A$ determinant. By using the Glasgow shell-model code,⁶ the wave functions are naturally expressed as a sum of Slater determinants, and hence, effects of antisymmetry are explicitly included. The πN amplitudes $h(q)$ are calculated using the usual partial-wave expansion; the πN phase shifts and inelasticity parameters used are from the 1987 analysis of Arndt.^{2,7} Necessary extensions of our previous methods⁵ for arbitrary partial waves are outlined in the appendix. The wave functions were obtained by using the Cohen-Kurath $2BME$ interaction,⁸ and the oscillator parameter was fixed by electron-scattering analyses. Thus our calculations involve no free parameters.

III. RESULTS WITHOUT ABSORPTION

Equation (1) may be formally rewritten as

$$F(q) = ike^{i\Delta M\pi/2} \int_0^{\infty} b db J_{\Delta M}(qb) \Gamma(b). \quad (5)$$

In Eq. (5), $\Delta M = M_i - M_f$, b is the impact parameter, and $\Gamma(b)$ is the nuclear profile function resulting from evaluating the nuclear matrix element. For zero-degree transitions, $q=0$ and the Bessel function in Eq. (5) is 1 for $\Delta M=0$ or 0 otherwise. The integral then reduces simply to an integration of the profile function over impact parameter. A graphical representation of $\Gamma(b)$ thus produces a useful, physical picture, and one may immediately ascertain the spatial origin of contributions to the forward angle transition.

In Fig. 1 the profile function for the reaction $^{14}\text{C}(\pi^+, \pi^0)^{14}\text{N}(0^+)$ is plotted for three different pion kinetic energies. The calculation assumed contributions from partial waves of $s, p, d,$ and f . The lowest energy, 180 MeV, is near the canonical value of the Δ resonance, while the other two energies are near the lowest and highest energies measured by Rokni *et al.*¹ As is well known, the dominant contributions to pion-induced SCX reactions near resonance energies arise from regions near the nuclear surface: At 180 MeV $\text{Re}\Gamma(b)$ has a maximum for a value of the impact parameter near the radius R . Relatively few of the pions that have impact parameters smaller than R survive. As one increases the pion energy more and more of the cross section arises from inside the nucleus, until at 600 MeV $\text{Im}\Gamma$ resembles the density distribution of the nucleus. Another change occurring between energies around the resonance and 600 MeV is that Γ has changed from being essentially a real

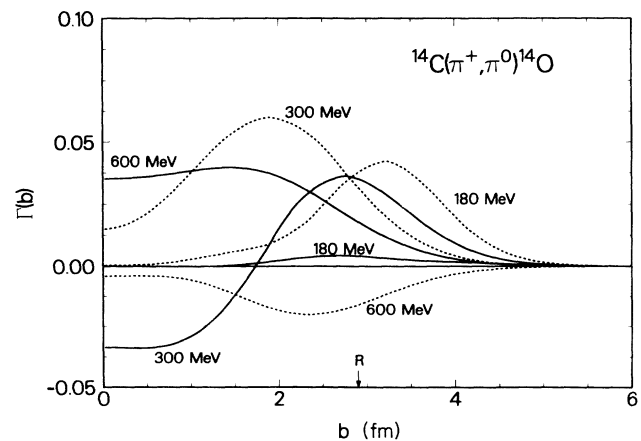


FIG. 1. Profile function $\Gamma(b)$ for the reaction $^{14}\text{C}(\pi^+, \pi^0)^{14}\text{N}(0^+)$ for three different pion kinetic energies: 160, 300, and 600 MeV. For each energy the solid curve is $\text{Im}\Gamma$ and the dashed curve is $\text{Re}\Gamma$.

function at resonance to essentially an imaginary function at 600 MeV.

In Fig. 2 are plotted zero-degree excitation functions for the $^{14}\text{C}(\pi^+, \pi^0)^{14}\text{N}(0^+)$ reaction showing the effects of including higher partial waves. Above 300 MeV kinetic energy it is clearly essential to include the d wave; about 450 MeV it is also necessary to include the f wave. The g and h waves are not statistically different from zero for energies below 600 MeV, and we do not include their contribution in the work below. The increasing cross section results from a competition between distortion—which is decreasing and which would result in a larger cross section—and the charge-exchange amplitude which is decreasing.

Also plotted in Fig. 2 are the experimental results of Rokni *et al.*¹ and Sennhauser *et al.*⁹ It is immediately apparent that the calculations appreciably overestimate the experimental SCX cross section. As already discussed in the Introduction, many higher-order processes have not been included in our calculation. The principal one of these is pion absorption on two or more nucleons. Below the resonance region two-body absorption has been found to be more important than absorption on three nucleons; from $T_\pi = 250$ to 400 MeV two- and three-body absorption are equally important;¹⁰ the importance of four-body absorption has also been estimated and found to be small.^{10,11} Some recent experiments¹² have shown that pion absorption on two and three nucleons have similar strengths around the resonance in qualitative agreement with the findings of Oset, Futami, and Toki.¹⁰ The Glauber distortion due to elementary πN processes [the factor $\prod_i (1 - \Gamma_i)$] is very important around the resonance and eliminates the contribution from small impact parameters, making the reaction rather peripheral as indicated above. With the intrinsic absorption probability on two and three nucleons roughly proportional to ρ^2 and ρ^3 , respectively (where ρ is the nuclear density), the effect of absorption at energies around the resonance should

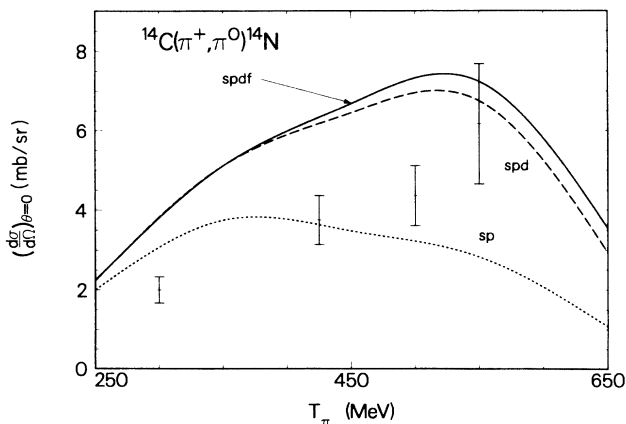


FIG. 2. Excitation function for the reaction $^{14}\text{C}(\pi^+, \pi^0)^{14}\text{N}(0^+)$ in the laboratory system calculated with three different assumptions regarding the number of contributing partial waves. The experimental points are from Rokni *et al.* (Ref. 1) and Sennhauser *et al.* (Ref. 9).

not be drastic. At higher energies the πN cross section decreases and the pions can penetrate more deeply into the interior of the nucleus. The absorption effects could then be more important. However, the decreasing strength of the absorption probability will have some compensating effects as we shall see.

IV. INCLUSION OF ABSORPTION

Glauber formalism, relying upon the on-shell πN scattering amplitude, neglects important pieces of an elaborate pion-nucleus optical potential, among which pion absorption plays a major role and must be included. If we recall the optical limit of Glauber theory,³ we have the distortion factor

$$\langle \Psi | \prod_i [1 - \Gamma_i(\mathbf{b} - \mathbf{s}_i)] | \Psi \rangle = \exp \left[-\frac{2\pi}{ik_{\text{c.m.}}} \int_{-\infty}^{\infty} dz f(q=0)\rho(\mathbf{b}, z) \right]. \quad (6)$$

Recalling the lowest-order pion-nucleus optical potential (in this paper we use the pion self-energy $\Pi = 2\omega V_{\text{opt}}$) is given by

$$\Pi^{(0)}(k, \rho(r)) = -4\pi \frac{\sqrt{s}}{m} f(q=0)\rho(r), \quad (7)$$

we have for the lowest-order approximation to the distortion factor

$$\text{DF}^{(0)} = \exp \left[-i \int_{-\infty}^{\infty} dz \frac{1}{2k} \Pi^{(0)}(k, \mathbf{b}, z) \right], \quad (8)$$

where $k = (\sqrt{s}/m)k_{\text{c.m.}}$ is the laboratory momentum. The complete distortion factor is written as

$$\text{DF} = \exp \left[-i \int_{-\infty}^{\infty} dz \frac{1}{2k} \Pi(k, \mathbf{b}, z) \right], \quad (9)$$

where $\Pi(k, \rho(b, z))$ is the full pion-nucleus self-energy. Hence missing from our calculated, standard Glauber distortion factor is the multiplicative factor

$$\text{DF}^{(2)} = \exp \left[-i \int_{-\infty}^{\infty} dz \frac{1}{2k} \Pi^{(2)}(k, \mathbf{b}, z) \right], \quad (10)$$

where $\Pi^{(2)}$ is the higher-order pion self-energy ($\Pi = \Pi^{(0)} + \Pi^{(2)}$). In Eq. (1) most of the contribution to the profile function comes from a narrow band of impact parameters $\Delta \approx b$ near the nuclear surface.⁵ Hence an estimate of the effect of the new distortion factor can be obtained by taking the value of $|\mathbf{b}|$ at the peak of the total A particle profile function in Eq. (5). This also tells us that the contribution from $\text{Re}\Pi^{(2)}$ will give rise to a phase in the amplitude of Eq. (1) with irrelevant consequences, while the contribution from $\text{Im}\Pi^{(2)}$ will produce a reduction which will account for the loss of pion flux into the reaction channels contained in $\text{Im}\Pi^{(2)}$ —dominantly pion absorption.¹³

By noting that the probability of reaction per unit length is given by

$$P = -\frac{1}{k} \text{Im}\Pi(k, \rho), \quad (11)$$

we see the square modulus of DF can be interpreted as the probability of survival of a pion with impact parameter \mathbf{b} to cross a nucleus without undergoing any reaction. Hence $|\text{DF}^{(2)}|^2$ will give us the probability that a pion crosses the nucleus with impact parameter \mathbf{b} without absorption. Thus, to include true absorption in our Glauber calculation, one must evaluate $\text{Im}\Pi^{(2)}(k, \rho)$.

The theoretical study in Oset, Futami, and Toki¹⁰ shows that at energies below the $\Delta(1232)$ resonance, two-body absorption accounts for most of the genuine absorption process (i.e., without initial- or final-state interaction). However, at energies around the Δ resonance and slightly above, three-body absorption becomes comparable with the two-body contribution. We shall denote by $\text{Im}\Pi^{(2,2)}$ the correction to the pion self-energy coming from the two-body absorption and by $\text{Im}\Pi^{(2,3)}$ the corresponding correction coming from three-body absorption.

We must now extend these results to energies above the resonance. For this purpose, we begin with the two-body

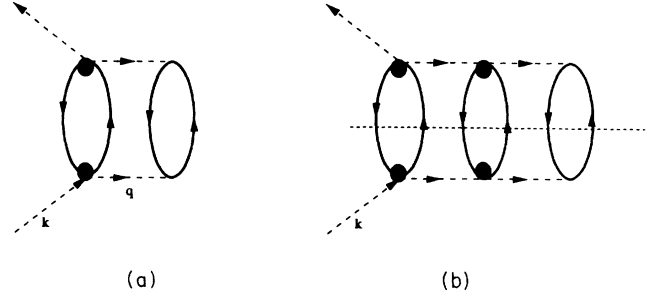


FIG. 3. Many-body diagrams exhibiting mechanisms for pion absorption through (a) two-particle two-hole and (b) three-particle three-hole excitations mediated by pion exchange.

absorption mechanism depicted in Fig. 3(a). The evaluation of this diagram in infinite nuclear matter when there is only pion exchange is equivalent to the one for the s -wave pion absorption that was worked out in detail in Garcia-Recio, Oset, and Salcedo.¹⁴ We obtain

$$\text{Im}\Pi^{(2,\pi)}(k) = -\int \frac{d^2q}{(2\pi)^3} \int_0^\infty d\omega \left[\frac{f}{\mu} \right]^2 F_\pi(q)^2 q^2 \frac{1}{4} \sum_{s_i, s_f, t_i, t_f} \sum_\lambda |T^\lambda|^2 \frac{1}{\pi} \theta(k^0 - \omega) \text{Im}U(\omega, \mathbf{k} - \mathbf{q}) \text{Im}U(q) D_0(q)^2 \Big|_{q^0 = k^0 - \omega}, \quad (12)$$

in analogy to Eq. (2.15) of Garcia-Recio, Oset, and Salcedo.¹⁴

In Eq. (12), f/μ is the ordinary πNN coupling constant ($f^2/4\pi = 0.08$), $F_\pi(q)$ is a monopole form factor for the πNN vertex ($\Lambda \approx 1300$ MeV),¹⁵ T^λ the πN scattering amplitude with λ the isospin of the final pion, s_i, s_f, t_i, t_f are the spin and isospin of the initial and final nucleons in the πN amplitude, $U(q)$ the Lindhard function for particle-hole (ph) excitation¹⁶ with the normalization of Oset and Palanques,¹⁷ and $D_0(q)$ the pion propagator. One can make use of the low-density approximation¹⁴ (suited for a peripheral problem like SCX) in which one makes the replacement

$$\text{Im}U(q) \xrightarrow{\rho \rightarrow 0} -\pi\rho\delta(|q^0| - q^2/2m), \quad (13)$$

with ρ the nuclear density and m the nucleon mass. An improved approximation¹⁴ which considers the Pauli blocking factor is unnecessary here, both because the relevant densities felt by the pion are small and because the energies of the nucleons after pion absorption are large. With this approximation and an angular average, we obtain

$$\text{Im}\Pi^{(2,\pi)}(k) = -\frac{1}{(2\pi)^2} m q^3 \left[\frac{f}{\mu} \right]^2 \times \frac{1}{4} \sum_{s_i, s_f, t_i, t_f} \sum_\lambda |T^\lambda|^2 \pi \rho^2 D_0(q)^2, \quad (14)$$

with

$$q^0 = k^0 - \frac{\mathbf{k}^2 + \mathbf{q}^2}{2m}, \quad (15)$$

and

$$q = \left[m \left[k^0 - \frac{\mathbf{k}^2}{2m} \right] \right]^{1/2}. \quad (16)$$

On the other hand, the amplitude T^λ is normalized such that in the c.m. system

$$\left[\frac{d\sigma}{d\Omega} \right]^\lambda = \left[\frac{m}{4\pi\sqrt{s}} \right]^2 \sum_{s_i, s_f} |T^\lambda|^2, \quad (17)$$

with $d\sigma/d\Omega$ the unpolarized πN differential cross section.

We shall now make an additional approximation that assumes a constant value for $|T^\lambda|^2$ equal to its average given by Eq. (17). Hence, by summing explicitly over the isospin λ of the final pion state and averaging over the initial nucleon isospin, we obtain

$$\frac{1}{4} \sum_{s_f, s_i, t_i, t_f} \sum_\lambda |T^\lambda|^2 = 4\pi \frac{s}{m^2} \bar{\sigma}, \quad (18)$$

with

$$\bar{\sigma} = \frac{1}{3}(2\sigma_{3/2} + \sigma_{1/2}), \quad (19)$$

in which the indices of σ denote the isospin of the πN system. Hence we have

$$\text{Im}\Pi^{(2,\pi)}(k) \approx - \left[\frac{f}{\mu} \right]^2 F_\pi(q)^2 \frac{s}{m} q^3 \bar{\sigma} D_0^2(q) \rho^2, \quad (20)$$

with q^0 given in Eq. (15).

This is an easy analytical expression that roughly takes into account the two-body absorption due to π exchange. However, in Oset, Futami, and Toki¹⁰ a more elaborate calculation was done which also took into account the exchange of the ρ meson and the indirect effect of correlations. In other words, effective longitudinal and transverse interactions were used instead of the bare one-pion exchange. The longitudinal effective interaction is given by $q^2 D_0(q) F_\pi(q)^2 + g'$ with $g' \approx 0.6-0.7$; hence it adds the Landau-Migdal parameter g' to the one-pion-exchange contribution. The transverse interaction is $q^2 D_\rho(q) F_\rho(q)^2 C_\rho + g'$, with D_ρ the ρ meson propagator, $F_\rho(q)$ is the ρNN form factor, and C_ρ is the ratio of the ρNN and πNN coupling constants squared. Both interactions are smooth functions of q . As a consequence, $q^2 D_0(q) F_\pi(q)^2$ in Eq. (20) should be replaced by an effective constant in a realistic calculation. The above considerations allows us to write

$$\text{Im}\Pi^{(2,2)}(k) \approx -D_2 \frac{s\bar{\sigma}}{q} \rho^2, \quad (21)$$

where we have also used the fact that $F_\pi(q)$ is a smooth function of q for $\Lambda = 1300$ MeV, with q defined above, and with s the square of c.m. energy for a pion of momentum k and a nucleon at rest, and $\bar{\sigma}$ the spin-isospin-averaged unpolarized πN cross section at this energy given in Eq. (19).

Equation (21) agrees remarkably well with the actual calculations of Oset, Futami, and Toki¹⁰ throughout the resonance region (at the level of 10%). This comparison allows one to extract the proportionality constant D_2 (chosen at $T_\pi = 300$ MeV):

$$D_2 = 1.16 \times 10^{-2} \text{ fm}^5 \text{ mb}^{-1}.$$

We now accept Eq. (21) as an extrapolation of two-body absorption to energies above the resonance region. The extrapolation correctly takes into account phase space, the strength of the πNN vertex, and the varying strength of the πN scattering amplitude. Of course, when we go away from the $\Delta(1232)$ resonance, we expect resonances other than the Δ —which is the only ingredient considered in Oset, Futami, and Toki¹⁰—to play a role in the πN scattering amplitude. In a picture where π and ρ couple to all these resonances and the ratio of coupling constants is kept constant (as is generally assumed for N and Δ), the extrapolation of Eq. (21) will hold.

This, together with the good reproduction of the actual results by Eq. (21) in a broad region of energies around resonance (in spite of the resonant and thus rapidly changing character of the πN cross section), gives us confidence in the extrapolation of Eq. (21) to higher energies, although we should expect the approximation to be less accurate as we go to very high energies.

For the three-body absorption, we follow a similar procedure. We start from the Feynman diagram of Fig. 3(b) where only pion exchange is used as a mediator. By following straightforward Feynman rules and then Cutkosky rules¹⁸ to evaluate the imaginary part coming when the three ph excitations are placed on shell [dotted cut in Fig. 3(b) corresponding to three-body pion absorption] and using the approximation of Eq. (18), we obtain

$$\begin{aligned} \text{Im}\Pi^{(2,3)}(\mu) \approx & -\frac{1}{\pi m^3} \left[\frac{f}{\mu} \right]^2 \rho^3 \int_0^{q_{\max}} q dq \int_{q'_{\min}}^{q'_{\max}} q'^3 dq' \int_{\cos\theta_{\min}}^{\cos\theta_{\max}} d \cos\theta D_0^2 \left[k^0 - \frac{(\mathbf{k}-\mathbf{q})^2}{2m}, q \right] D_0^2 \left[\frac{q'^2}{2m}, q' \right] F^2 \left[\frac{q'^2}{2m}, q' \right] \\ & \times s(k^0) \bar{\sigma}(k^0)_s \left[k^0 - \frac{(\mathbf{k}-\mathbf{q})^2}{2m} \right] \bar{\sigma} \left[k^0 - \frac{(\mathbf{k}-\mathbf{q})^2}{2m} \right], \end{aligned} \quad (22)$$

with

$$\cos\theta = \hat{\mathbf{k}} \cdot \hat{\mathbf{q}},$$

and

$$q_{\max} = \frac{2k + (12k^0 m - 2k^2)^{1/2}}{3}, \quad (23)$$

$$q'_{\max} = q'_4, \quad (24)$$

$$q'_{\min} = \begin{cases} \max[0, q'_3] & \text{for } \Delta_1 \leq 0 \\ \max[0, q'_2, q'_3] & \text{for } \Delta_1 > 0, \end{cases} \quad (25)$$

$$q'_{\min} = \begin{cases} \max[0, q'_3] & \text{for } \Delta_1 \leq 0 \\ \max[0, q'_2, q'_3] & \text{for } \Delta_1 > 0, \end{cases} \quad (26)$$

where

$$\Delta_1 = 4k^0 m - 3q^2 - 2k^2 - 4kq, \quad (27)$$

$$\Delta_2 = 4k^0 m - 3q^2 - 2k^2 + 4kq, \quad (28)$$

$$q'_2 = \frac{-q + \sqrt{\Delta_1}}{2}, \quad (29)$$

$$q'_3 = \frac{q - \sqrt{\Delta_2}}{2}, \quad (30)$$

$$q'_4 = \frac{q + \sqrt{\Delta_2}}{2}. \quad (31)$$

Similarly,

$$\cos\theta_{\min} = \max[-1, A], \quad (32)$$

$$\cos\theta_{\max} = \min[1, B], \quad (33)$$

with

$$A = \frac{m}{kq} \left[-\frac{qq'}{m} + \frac{k^2}{2m} + \frac{q^2}{m} + \frac{q'^2}{m} - k^0 \right], \quad (34)$$

$$B = \frac{m}{kq} \left[\frac{qq'}{m} + \frac{k^2}{2m} + \frac{q^2}{m} + \frac{q'^2}{m} - k^0 \right]. \quad (35)$$

A word of caution must be raised when evaluating Eq. (22) as the first pion propagator can appear on shell. This is possible because the first ph excitation on the left in Fig. 3(b) can be physically excited, with a real pion in the final state (quasielastic scattering), which is then absorbed by two nucleons [the two ph excitations on the right of Fig. 3(b) are placed on shell]. Salcedo *et al.*¹⁹ show that such contributions can be interpreted as the probability of quasielastic scattering followed by the probability that the scattered pion is absorbed by two nucleons during its lifetime in the elastic channel (that is, its lifetime without undergoing quasielastic or two-body absorption). Such a contribution should not be included here because events with a quasielastic step are already removed from the elastic channel by the Glauber distortion factor $\langle |\prod(1-\Gamma)| \rangle$. This is why the relevant quantity is called genuine three-body absorption¹⁹ which would come from ingredients of the interaction other than pion exchange. We should note that the second pion propagator in Eq. (21) corresponding to the pions on the right in Fig. 3(b), as well as the pions in Fig. 3(a), are necessarily off shell because a real pion cannot excite a physical ph excitation, or equivalently a pion cannot be absorbed by a single nucleon in nuclear matter.

By following steps similar to those carried out in the two-body absorption case when replacing $q^2 D_0(q) F_\pi(q)^2$ by a constant and taking into account the phase space in the integrations, one can also find a useful and handy approximation²⁰ given by

$$\text{Im}\Pi^{(2,3)}(k) \approx -D_3 \frac{s\bar{\sigma}}{q'} \frac{s'\bar{\sigma}'}{q'} \rho^3, \quad (36)$$

with

$$q' = \left[\frac{m}{2} \left(k^0 - \frac{\mathbf{k}^2}{2m} \right) \right]^{1/2}, \quad (37)$$

and $s', \bar{\sigma}'$ calculated at $T'_\pi = \frac{2}{3} T_\pi$. Once again, when this is contrasted with the actual results of Oset, Futami, and Toki,¹⁰ we see that Eq. (36) also holds to within 10% in the range between $T_\pi = 200$ and 300 MeV. At the same time, this comparison provides the value of D_3 :

$$D_3 = 1.15 \times 10^{-7} \text{ fm}^8 \text{ mb}^{-2} \text{ MeV}^{-1}. \quad (38)$$

Once again, and for the same reasons given above, we take Eq. (36) as the extrapolation of three-body absorption to higher energies.

With all these ingredients we can now write down the expression for the additional distortion factor due to pion absorption:

$$DF^{(2)}(\mathbf{b}) = \exp \left[- \int_{-\infty}^{\infty} [C_2 \rho^2(\mathbf{b}, z) + C_3 \rho^3(\mathbf{b}, z)] dz \right], \quad (39)$$

with $C_2 = (1/2k) D_2 s \bar{\sigma} / q$ and $C_3 = (1/2k) D_3 (s \bar{\sigma} / q') s' \bar{\sigma}' / q'$ where we have made use of the local-density approximation [$\rho \rightarrow \rho(r)$] to go from infinite matter to finite nuclei. Furthermore, in order to incorporate the finite range of the interaction and, hence, improve the local-density approximation, we have considered the finite range of the absorption pieces as done in Salcedo *et al.*¹³ in the resonance region, thus replacing $\rho^n(r)$ in Eq. (39) by

$$\rho^n(r) \rightarrow \left[\frac{k^2}{2\pi} \right]^{3/2} \int d^3 r' \rho^n(r') e^{-(1/2)(r-r')^2 k^2},$$

where k is the pion momentum.

V. RESULTS AND DISCUSSION

In Fig. 4 we show the coefficients C_2 and C_3 in arbitrary units as a function of the pion kinetic energy T_π . Both C_2 and C_3 are decreasing functions of the energy in the range of energy shown. The coefficient C_2 decreases by a factor of 15 from $T_\pi = 200$ to 600 MeV, while C_3 decreases by about a factor of 45 in the same energy range. This is a consequence of moving away from the resonance where the cross section σ and hence the coefficients C_2 and C_3 have their maximum value. Because C_3 contains σ twice and C_2 only once, the falloff of C_3 is more pronounced than that of C_2 . In Rokni *et al.*¹ pion absorption was introduced phenomenologically by means of a factor like the one in Eq. (39) albeit with $C_3 = 0$ and C_2 equal to a constant subsequently fit to experiment. The results of our work indicate that—apart from the appearance of a three-body term—the coefficient C_2 is very dependent on energy.

We use shell-model wave functions for ¹⁴C and ¹⁴N with an oscillator parameter $\alpha^2 = 0.40 \text{ fm}^{-2}$ [the radial wave functions $\sim \exp(-\frac{1}{2}\alpha^2 r^2)$] obtained from electron

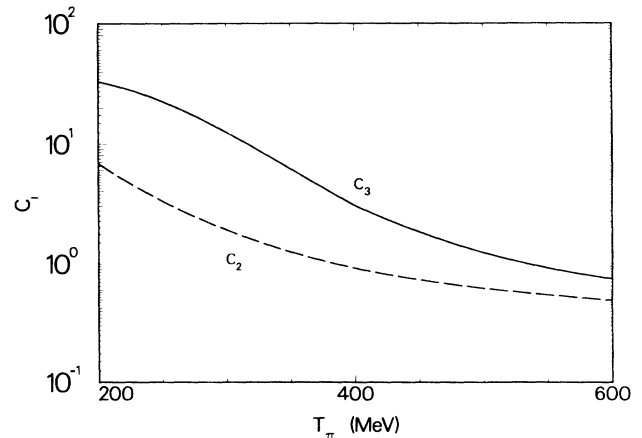


FIG. 4. Plot of the calculated values of the coefficients C_2 and C_3 , in units of fm^5 and fm^8 , respectively, appearing in Eq. (39) and which account for two- and three-body pion absorption as a function of pion kinetic energy.

scattering²¹ with the removal of effects due to the finite size of the proton. A simplified three-parameter Fermi density²¹ was assumed for the density appearing in the expressions for the absorption distortion factor of Eq. (39).

In Fig. 5 are shown the results for $d\sigma/d\Omega$ at $\theta=0$ for the $^{14}\text{C}(\pi^+, \pi^0)^{14}\text{N}(0^+)$ reaction including effects of pion absorption. As anticipated, the role of absorption is to decrease the cross section. The effects are not large. Inclusion of two-body absorption reduces the cross section by about 10% at $T_\pi=300$ MeV and by 5% at $T_\pi=550$ MeV. The additional inclusion of three-body absorption makes the total reduction due to pion absorption approximately 15% at $T_\pi=300$ MeV and 6% at $T_\pi=550$ MeV. As the pion energy increases, the effect of pion absorption is further reduced. Our results are about 40% above the experimental errors at $T_\pi=300$ MeV, 33% in the region of $T_\pi=400$ –500 MeV, and are compatible with experiment at $T_\pi=550$ MeV.

It is interesting to remark on the moderate role played by pion absorption in the entire range of energies studied. As discussed above, if there were a constant absorption probability, i.e., $C_2=\text{const}$, $C_3=\text{const}$, we would have expected a more important role for absorption above resonance than around the resonance and with a larger reduction factor around 400–500 MeV than around 250 MeV. The role of the absorption factor is to account for the elimination of the contribution from small impact parameters. However, if this contribution has already been eliminated by the ordinary Glauber distortion factor, there is little role remaining for the additional distortion factor due to absorption. However, at energies above resonance where the πN cross section is drastically reduced, the usual Glauber distortion factor reduces the small-impact-parameter components much less than at resonance and the role of absorption can be seen. This is seen clearly in Rokni *et al.*¹ where $C_2=\text{const}$, $C_3=0$. They find moderate reduction factors around 250 MeV, but a reduction factor of about 3 around 400–500 MeV. Their simplified version of the Glauber approach produces a

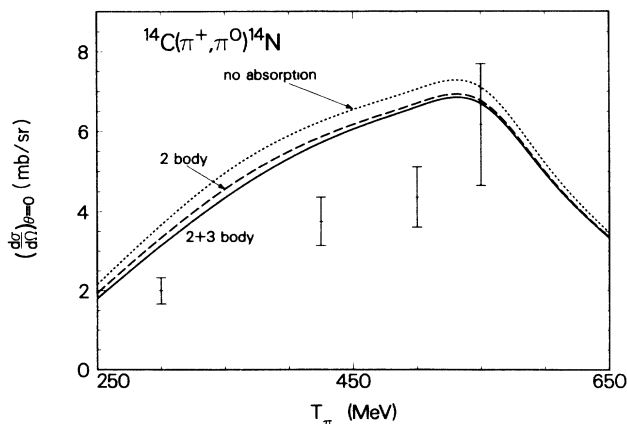


FIG. 5. Excitation function for the reaction $^{14}\text{C}(\pi^+, \pi^0)^{14}\text{N}(0^+)$ in the laboratory system calculated with the inclusion of pion absorption. Partial waves up to and including $l=3$ were used.

shape for the cross section before absorption quite different than ours with discrepancies with experiment of about a factor of 3 in the energy region of 400–500 MeV before they include the extra reduction factor. As a consequence, a distortion factor with $C_2=\text{const}$ and fitted to experiment brings the calculated results in near agreement with experiment in the energy range of the figure.

Our theoretical results without the effects of distortion follow the experimental shape of the cross section with approximately a 40–50% overestimate in the entire energy range (the last point at 550 MeV fits within the large experimental error bars). The effect of absorption brings the discrepancy to about 33%, and the resulting shape also follows the experimental trend. Had we employed a constant absorption probability consistent with the values chosen at 250 MeV, we would have obtained a shape much different than experiment. In our case the greater chance of absorption to reduce the cross section at energies above resonance are more than compensated by the drastic decrease with energy of the absorption probabilities.

Obviously, it would be very interesting to perform experiments on pion absorption in this energy region to determine if they support the decrease in absorption with increasing pion kinetic energy as predicted. (One should note, however, that the absorption cross is not simply proportional to the value of the coefficients C_2 and C_3 ; rather, a careful calculation must be performed.¹⁹)

One might still be concerned about the remaining discrepancy between experiment and our theoretical calculation. However, the fact that the shape is approximately correct and that the ratio of theoretical and experimental cross section is approximately constant suggests an overall normalization factor. Indeed, such a factor may occur for several reasons. We have used the same harmonic-oscillator parameter for ^{14}C and ^{14}N ; this implies complete overlap of the wave functions of the core nucleons. However, the experimental values of the harmonic-oscillator parameters differ by 2%,²¹ although this difference is compatible with experimental errors of the parameters.

However, a straightforward calculation suggests this may not produce a significant change. The problem may be approached by expanding one oscillator function in terms of another with a different spring constant. If one function has the factor $\exp(-\frac{1}{2}\alpha^2 r^2)$ and the second $\exp(-\frac{1}{2}r^2)$, then their overlap is $[2\alpha/(1+\alpha^2)]^{l+3/2}$ (each function having $n=1, l$). Clearly, this effect should be small, although it is conceivable that additional, large cancellations could occur from the $n \neq 1$ terms in the expansion. We have performed an explicit calculation by numerically integrating each of the single-particle profile functions in the $A \times A$ determinant and find the effect to be less than 2%.

The effect of spin flip (both isoscalar and isovector) on the analog transition has also been calculated. *A priori* one would expect the effect of spin flip on the zero-degree cross section to be small for two reasons: First, in a single-scattering approximation, spin flip is zero at 0° and thus spin flip can only contribute through the effects of

distortion. Second, both the 0^+ ground state ^{14}C and the analog state are nearly pure $S=0$ eigenstates; therefore, a single spin-flip process cannot contribute to this transition at any angle. We have calculated the maximum effect to be around 550 MeV where it increases the forward angle cross section by 2%. Increasing or decreasing the pion kinetic energy reduces the contribution of spin flip to the ^{14}N cross section.

In Fig. 6 we show the results for the reaction $^7\text{Li}(\pi^+, \pi^0)^7\text{Be}$ (using $\alpha^2=0.371$) including the effects of absorption and compare them with the experimental results of Rokni *et al.*¹ The effects of spin flip could conceivably be larger here than in the ^{14}C reaction since the ^7Li ground state has $S=\frac{1}{2}$ and therefore spin flip is not excluded by angular momentum selection rules (although one might still expect it to be small at forward angles). Indeed, the spin-flip contribution increases the forward angle cross section by 10% at the lower energies and $\approx 5\%$ at the highest energy, somewhat larger than in the case for ^{14}C , but still relatively unimportant. Once again one observes that our results are systematically 20% above experimental errors. We also note in this case the role played by pion absorption is somewhat smaller than for ^{14}C , producing reduction factors of only 5–10%. This suggests that the role played by absorption is much more important in heavier nuclei.

We have also calculated these reactions using the new, 1989 phase-shift analysis of Arndt and Roper.⁷ We found the theoretical cross section for the SCX reaction to increase by $\approx 5\%$ at 550 MeV. Thus additional π - N scattering experiments are required throughout this energy region to better determine the phase shifts, particularly the higher partial waves.

The trend of the effects of absorption is to decrease with increasing pion energy. As a consequence, the ordinary Glauber picture—relying upon πN scattering data—will become more reliable as the pion energy increases. It will provide an attractive theoretical framework for a microscopic study of high-energy pion-nucleus reactions.

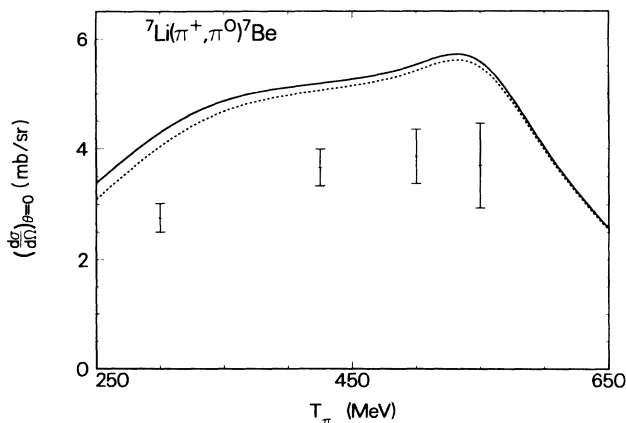


FIG. 6. Excitation function for the reaction $^7\text{Li}(\pi^+, \pi^0)^7\text{Be}$ in the laboratory system calculated with the inclusion of pion absorption.

VI. CONCLUSION

We have used in this paper a microscopic model based on the Glauber theory of multiple scattering to study the SCX reaction above the (3,3) resonance. Our results for ^7Li and ^{14}C follow closely the shape of the experimental data, but exceed experiment by about 25% and 33%, respectively. The standard Glauber theory was modified to include pion absorption. The evaluation of the absorption probability relied upon detailed work around the resonance and which is compatible with experimental cross sections. The extrapolation of these results to energies above the resonance was performed assuming a model similar to those used around the resonance and including the modification of phase space with energy. The result was a decreasing function of the absorption probability on two and three nucleons as the pion energy increased. This absorption probability resulted in reductions of the cross section by a small amount for ^7Li and 6–15% for ^{14}C , implying that the effects of absorption become increasingly important for heavier nuclei. We have also found that as the energy increases, the effects of pion absorption on the SCX cross section become less important. This further suggests that Glauber theory will become increasingly accurate as the pion energy increases.

The reliability of Glauber theory at higher energies is based, in part, on a decreased role played by absorption. As one goes away from resonance, our extrapolation is also less reliable. It is therefore very important to perform experiments on pion absorption at high energies to test these theoretical predictions and then to set limits on the importance of such many-body processes can have on different pion-nucleus reactions. This information is needed not only for the current work, but also in other aspects of physics such as photonuclear reactions, antiproton annihilation, and heavy-ion reactions. The experimental investigation of pion absorption should be considered of high priority in the next phase of experiments on pion-nucleus reactions at high energies.

APPENDIX

In previous work^{5,22} we have detailed the method we use to calculate the single-particle profile function and from thence to the many-body determinant. However, in these earlier papers the energies were sufficiently low that we restricted the partial waves to be zero and one. Here we briefly indicate the generalization to an arbitrary number of partial waves.

The non-spin-flip amplitudes are obtained from

$$f(q) = \sum_l [(l+1)f_{l+} + lf_{l-}] P_l(\cos\theta), \quad (\text{A1})$$

where the f_l are defined for each channel J, I by

$$f_{JI} = \frac{\eta_{JI} e^{2i\delta_{l,J,I}} - 1}{2ik}, \quad (\text{A2})$$

with J, I the total spin and isospin and the η_{JJ} are the inelasticities. The momentum transfer q is related to the angle of scattering through the relation $\cos\theta = 1 - q^2/2k^2$. Thus the scattering amplitude may be

rewritten as a polynomial in q^2 , $f(q) = \sum A_n q^{2n}$, the coefficients of which are determined once the phase shifts and inelasticities are specified. The single-particle profile function

$$\langle n'l'j'm' | \Gamma(\mathbf{b}-\mathbf{s})nljm \rangle = \sum_n A_n \frac{1}{2\pi i k} \int d^2q e^{-iq \cdot \mathbf{b}} q^{2n} \langle n'l'j'm' | e^{iq \cdot \mathbf{s}} | nljm \rangle$$

may now be evaluated either numerically using the techniques of Oset and Strottman²² or, if the single-particle wave functions are harmonic-oscillator functions, by use of the analytic expression of Oset and Strottman.²³

It remains to relate the coefficients A_n to the individual partial-wave amplitudes. The relation between the A_n and the non-spin-flip amplitudes f_l may be obtained by using Rodrigues' formula for the Legendre functions and a certain amount of algebraic manipulation:

$$A_n = \frac{(-1)^n}{(2k^2)^n} \frac{(2n)!}{2^n(n!)^2} \sum_{l=n} \frac{(l+n)!}{(2n)!(l-n)!} f_l. \quad (\text{A3})$$

The non-spin-flip amplitudes are obtained from

$$g(q) = \sum_l (f_{l+} - f_{l-}) P'_l(\cos\theta) \sin\theta. \quad (\text{A4})$$

If one assumes $\sin\theta \approx q/k$, one may evaluate the following required expressions:

$$\langle n'l'j'm' | \Gamma(\mathbf{b}-\mathbf{s})nljm \rangle = \sum_n B_n \frac{1}{2\pi i k} \int d^2q e^{-iq \cdot \mathbf{b}} q^{2n+1} \langle n'l'j'm' | e^{iq \cdot \mathbf{s}} i\sigma \cdot \hat{\mathbf{n}} | nljm \rangle, \quad (\text{A5})$$

with coefficients

$$B_n = \frac{(-1)^{n+1}}{k(2k^2)^n} \frac{(2n+2)!}{2^{n+1}(n!)(n+1)!} \sum_{l=n+1} \frac{(l+n+1)!}{(2n+2)!(l-n-1)!} g_l. \quad (\text{A6})$$

The integral appearing in Eq. (A5) may be evaluated using the formulas of Oset and Strottman.²²

¹S. Rokni *et al.*, Phys. Lett. B **202**, 35 (1988).

²R. A. Arndt, J. M. Ford, and L. D. Roper, Phys. Rev. D **32**, 1085 (1985).

³R. J. Glauber, *Lectures in Theoretical Physics* (Interscience, New York, 1959), Vol. 1, pp. 315-414.

⁴E. Oset *et al.*, in *Pion-Nucleus Physics: Future Directions and New Facilities at LAMPF*, Proceedings of the Los Alamos Conference on Pion-Nucleus Physics, AIP Conf. Proc. No. 163, edited by R. J. Peterson and D. D. Strottman (AIP, New York, 1988).

⁵E. Oset and D. Strottman, Nucl. Phys. A **355**, 437 (1981).

⁶R. R. Whitehead, A. Watt, B. J. Cole, and I. Morrison, in *Advances in Nuclear Physics*, edited by M. Baranger and E. Vogt (Plenum, New York, 1978), Vol. 10.

⁷R. A. Arndt and L. D. Roper, SAID computer program (unpublished).

⁸S. Cohen and D. Kurath, Nucl. Phys. **78**, 1 (1965).

⁹U. Sennhauser *et al.*, Phys. Rev. Lett. **51**, 1324 (1983).

¹⁰E. Oset, Y. Futami, and H. Toki, Nucl. Phys. A **448**, 597 (1986).

¹¹T. Yasuda and H. Toki, Prog. Theor. Phys. **77**, 905 (1987).

¹²G. Backenstoss *et al.*, Phys. Lett. B **222**, 7 (1989); S. D. Hy-

man *et al.*, Phys. Rev. C **41**, R409 (1990); D. Mack, contribution to PANIC, MIT, June 1990 (unpublished).

¹³L. L. Salcedo, E. Oset, M. G. Vicente-Vacas, and C. Garcia-Recio, Nucl. Phys. A **484**, 557 (1988).

¹⁴C. Garcia-Recio, E. Oset, and L. L. Salcedo, Phys. Rev. C **37**, 194 (1988).

¹⁵R. Machleidt, K. Holinde, and Ch. Elster, Phys. Rep. **179**, 1 (1987).

¹⁶A. L. Fetter and G. D. Walecka, *Quantum Theory of Many Particle Systems* (McGraw-Hill, New York, 1971).

¹⁷E. Oset and A. Palanques, Nucl. Phys. A **359**, 289 (1981).

¹⁸C. Itzykson and J. B. Zuber, *Quantum Field Theory* (McGraw-Hill, New York, 1980).

¹⁹L. L. Salcedo, E. Oset, D. Strottman, and E. Hernandez, Phys. Lett. B **208**, 339 (1988).

²⁰E. Hernandez, Ph.D. thesis, University of Valencia, 1988 (unpublished).

²¹H. De Vries, C. W. de Jager, and C. de Vries, At. Data Nucl. Data Tables **36**, 495 (1987).

²²E. Oset and D. Strottman, Nucl. Phys. A **377**, 297 (1982).

²³E. Oset and D. Strottman, At. Data Nucl. Data Tables **28**, 531 (1983).